Published in final edited form as:

Small Methods. 2018 March 13; 2(3): . doi:10.1002/smtd.201700318.

Micro- and Macrobioprinting: Current Trends in Tissue Modeling and Organ Fabrication

Dr. Marco Santoro, **Javier Navarro**, and **John P. Fisher [Prof.]**

Fischell Department of Bioengineering University of Maryland, 3238 Jeong H. Kim Engineering Building, College Park, MD 20742, USA,

Center for Engineering Complex Tissues, University of Maryland, 3238 Jeong H. Kim Engineering Building, College Park, MD 20742, USA

Abstract

The recapitulation of human anatomy and physiology is critical for organ regeneration. Due to this fundamental requirement, bioprinting holds great promise in tissue engineering and regenerative medicine due to the possibility of fabricating complex scaffolds that host cells and biochemical cues in a physiologically relevant fashion. The ever-growing research in this field has been proceeding along two different, yet complementary, routes: on the one hand, the development of bioprinting to fabricate large tissue surrogates for transplantation purposes in vivo (macrobioprinting), and on the other the spread of bioprinting-based miniaturized systems to model the tissue microenvironment in vitro (microbioprinting). The latest advances in both macro- and microbioprinting are reviewed, emphasizing their impact on specific areas of tissue engineering. Additionally, a critical comparison of macro- versus microbioprinting is presented together with advantages and limitations of each approach. Ultimately, findings obtained both at the macro-and microscale are expected to provide a deeper insight in tissue biology and offer clinically relevant solutions for organ regeneration.

Keywords

bioprinting; complex tissues; organ-on-a-chip; regenerative medicine; tissue engineering

1. Introduction

Tissue engineering (TE) and regenerative medicine have made remarkable progress in the last decades toward the creation of functional tissues and organ surrogates. Among the technological breakthroughs behind these advances, 3D bioprinting holds great promise in the fabrication of physiologically relevant scaffolds that capture the complex anatomy and physiology of native tissues, overcoming the limitations of conventional fabrication techniques for scaffolds.[1,2]

The ORCID identification number(s) for the author(s) of this article can be found under https://doi.org/10.1002/smtd.201700318.

Conflict of Interest

The authors declare no conflict of interest.

The classic definition of bioprinting refers to the subclass of 3D printing technologies tailored for the use of biomaterials, cells, and biomolecules as printing resins for scaffold fabrication, commonly referred as “bioinks.”[3] Another definition that has been reported focus on the development of organ surrogates as the central goal of bio-printing, and thus define it as “the printing and patterning in 3D of all the components that make up a tissue (cells and matrix materials) to generate structures analogous to tissues.”[4] Despite these minor differences, the core definition of bioprinting involves the deposition of biomaterials and organ components (cells, growth factors, and/or extracellular matrix (ECM)) in a single step, and therefore should be separated from the manufacturing of biocompatible scaffolds followed by cell seeding, which should still be considered as 3D printing.

Similar to other 3D printing techniques, bioprinting allows for high spatiotemporal control over the simultaneous deposition of materials with different composition, spatial distribution, and architectural accuracy according to a computer-aided design (CAD). Three different bioprinting approaches exist to recapitulate tissue properties and functions: autonomous self-assembly, biomimicry, and the use of mini-tissues as elemental scaffold components.[3] The autonomous self-assembly approach is based on developmental biology principles, where cells are the primary drivers for tissue composition, spatial organization, and physiology. Accordingly, in this approach bioprinting is used to deposit single cells and/or multicellular aggregates in order to mimic developing tissues in the early stages of embryogenesis. On the other hand, biomimicry-based approaches focus on reproducing distinctive tissue components (e.g., extracellular matrix gradient composition in articular cartilage or the branched pattern of vasculature) with a microscopic level of details to accurately recreate in vitro the tissue morphology observed in vivo. Finally, a third bioprinting strategy is based on the use of mini-tissues as building blocks for whole-organ regeneration. This approach is based on the notion that several tissues are made of smaller functional subunits, such as osteons in bones or nephrons in kidneys. Likewise, bioprinting is here focused on fabricating mini-tissues and assembling them in an anatomically relevant fashion.

Recently, bioprinting has also been leveraged for the fabrication of microfluidic devices, avoiding the time-consuming steps associated with conventional UV lithography of poly(dimethylsiloxane) (PDMS).[5] This development has paved the way for the design of bioprinting-based tissue models.[5–8] In return, these advances have raised even greater interest in bioprinting, as witnessed by the increasing number of publications in this area.[9] Numerous publications have emerged on this subject, with comprehensive reviews on bioprinting for tissue engineering[2,10,11] as well as dedicated reviews on bioprinting technologies,[12,13] selection of bioink,[13–15] and tissues/applications.[6,8,16–20]

Here, we will specifically focus on the latest progress made in the fields of tissue engineering and regenerative medicine related to bioprinting, regardless of the technology, the material, or the tissue/organ selected. In doing so, we will show the emerging dichotomy in bioprinting-based tissue engineering strategies, that is, the fabrication of macroscale constructs for large tissue regeneration (macrobioprinting) versus the development of microscale systems for tissue modeling (microbioprinting). We will present advantages of disadvantages of each strategy and emphasize how findings on the microscale level correlate

to those obtained at the macroscale, and their impact on future developments in tissue engineering and regenerative medicine.

2. Macro- and Microbioprinting

All fields of engineering apply basic science in two distinct ways, either for: (i) the development of commercial products for common use, or (ii) the fundamental study of a particular phenomenon. The distinction can be blurry, as the second category usually provides new knowledge that molds and optimizes the first. TE is not any different. Correspondingly, TE is broadly divided into the development of constructs that are meant to directly solve a medical need, or the modeling of physiologic and pathologic phenomena to elucidate basic biological mechanism. Here, we explore this dichotomy from the point of view of bioprinting, categorizing recent literature in bioprinting into macrobioprinting and microbioprinting. We completed this categorization based on the following criteria:

1. Macrobioprinting applications state a medical need to fulfill and aim to develop viable tissue constructs that can be transplanted into patients. These constructs are proposed as large-scaled (>20 mm^3), to fulfill anatomical dimensions, and there is no explicit concern about microscopic features within the bioprinted scaffolds, unless it has a critical impact on the construct performance. These approaches are generally published with in vivo characterization, congruent with the overall medical end goal. We also include studies reported as being during in vitro stages of development, if their overall goal is medical transplantation.
2. Microbioprinting encompasses the application of bioprinting techniques at micro- and nanometer scale for the development of miniaturized devices for tissue modeling and interrogation of the cell microenvironment. These studies are focused on the development of highly detailed tissue models, understanding the interaction between cells and their tissue-specific niche. To this end, this category heavily relies on the production of micro- and nanoscale features for in vitro investigations, although a few examples but some have been extended into in vivo stages with the objective of further understanding the physiologic phenomena or the model validity.

Our primary categorization parameter is the end goal of the study discussed (implantable scaffold vs tissue model) rather than the technology used and/or the tissue investigated. As an example, in the next section we will present two studies in which the same bioprinting process, bioink, and cell source were used.[21,22] Yet, one investigation aimed at producing a “fully cellularized skin equivalent for the future treatment of burn patients,” while the latter presented “skin tissue constructs [that] serve as 3D cell-based models to study ex vivo cell and tissue functions or milieu-/disease-dependent mechanisms.” Although the scaffolds produced are very similar, the end application and fundamental questions asked with each construct are different (macro- and microbioprinting, respectively). Ideally, the microbioprinted model can provide better knowledge on skin physiology, dwelling on the fundamental questions, and as it exploits the same technology and components applied to macrobioprinting, it can be used to further optimize and correct the macrobioprinted constructs.

3. Macrobioprinting for Large Organ Regeneration

Bioprinting holds great promise for the fabrication of scaffolds of clinically relevant size and physiological complexity due to the high spatiotemporal control over cell/material placement. However, size and complexity significantly vary between organs—for example, bone or skin may be quantified in meters or centimeters, but their structure and composition present microscopic features. As defined before, macrobioprinting is the fabrication of large constructs for the clinical regeneration of tissues regardless of the presence of microscopic features within the bioprinted scaffolds.

Several TE fields have incorporated macrobioprinting to advance their efforts; for example, the need for improved musculoskeletal tissue repair strategies of critically sized defects has greatly advanced macrobioprinting technologies.[11,23] Daly et al. designed load-bearing cartilage scaffolds that serve as tissue precursor for the formation of a whole bone in vivo (Figure 1A–C).[24] Here, the complete vertebrae of a human skeleton model was laser-scanned and bioprinted using poly(caprolactone) (PCL) for mechanical stability, and an alginate hydrogel loaded with mesenchymal stem cells (MSCs) for enhanced cellular recognition and adhesion. Once chondrogenically primed in vitro, the bioprinted construct supported hypertrophic cartilage formation in vivo, which ultimately served as a stepping stone for endochondral bone formation.[24] The combination of hydrogel with thermoplastic polymers (e.g., PCL) is an emerging trend in bioprinting to improve the scaffold overall mechanical properties. While Daly opted for a self-assembly bioprinting approach, Shim et al. followed a biomimetic approach to recapitulate cartilage anatomy and intratissue gradients. In this work, a multihead extrusion bioprinter was used to mimic the distinctive compositional gradient observed in the osteochondral region.[25] The same research group further developed this platform to produce multilayered constructs of 100 mm^3 that promoted both osteogenesis (MSCs and bone morphogenetic protein-2 (BMP-2) in collagen) and chondrogenesis (MSCs and transforming growth factor-β3 (TGF-β3) in hyaluronic acid (HA)).[26] The use of extrusion-based bioprinting to engineer heterogeneous tissues, such as the bone–cartilage interface, resulted in successful osteochondral tissue repair in a rabbit knee joint. Along this direction, the inclusion of ECM components and growth factor gradients in bioprinted patterns is an alternative strategy used to engineer the bone–cartilage interface.[26–29] Gurkan et al. engineered fibrocartilage via droplet-based bio-printing of MSCs in the presence of BMP-2 and TGF-β1. The biochemical gradients accurately modeled the anisotropic architecture of fibrocartilage normally observed at the bone–tendon interface.[27] Similarly, Mao and co-workers bioprinted anatomically accurate human meniscus scaffolds for controlled release of growth factors.[28] This approach enabled fabrication of 2.25 cm^3 scaffold for testing in a sheep model, where full restoration of both functional and biomechanical properties was demonstrated. Finally, Levato et al. fabricated ECM-containing osteochondral constructs (16 mm diameter, 5 mm height) that could be further scaled up for clinical use.[29] Given these successes in restoring cartilage anatomy and physiology in vivo, we envision that in the next decade macrobioprinting-based strategies will likely provide effective solutions for the clinical treatment of cartilage defects.

The inclusion of a synthetic polymer (e.g., PCL) is a prevalent strategy to enhance the mechanical strength of bioprinted constructs, as shown in the previous section. It follows

that this choice becomes even more essential for load-bearing tissues like bones, as shown in the fabrication of a 300 mm^3 bone scaffold via macrobioprinting of alginate/PCL by Kim and co-workers.[30] The work of Atala and co-workers provides the best example of the versatility of macrobioprinting for producing large constructs for in vivo reconstruction. In this landmark publication, the authors patterned different hydrogels within a mechanically stable PCL network and fabricated mandible and calvarial bone defects, skeletal muscles, and full-size human ears (Figure 1D–H).[31] Considering that the same bioprinter and material were used in all applications, the choice of the hydrogel bioink (cell source, ECM inclusion, etc.) directed tissue regeneration. In other words, a robust in vivo response is simultaneously driven by: (i) the presence of the appropriate biological cues, given by the bioink selection, and by (ii) anatomically relevant spatial presentation provided by the bioprinting process.

The multihead printing process also involved the deposition of a sacrificial material (Pluronic F-127) that could be easily washed out upon bioprinting, resulting in the creation of microchannels permissive to nutrient diffusion and tissue ingrowth.[31] Although this design supported cell viability, tissue homeostasis is primarily driven by the presence of a vascular network within the newly formed tissue. Accordingly, the development of vascularization strategies is imperative for the successful fabrication of large tissues and represents a central challenge in TE.[32,33] A significant contribution in this field has been certainly made by Khademhosseini and co-workers. Based on the notion that angiogenesis and osteogenesis evolve simultaneously within the osteoblastic niche,[34,35] Khademhosseini and co-workers recapitulated the complex architecture of native bone together with its microvasculature, where the presence of a perfusable vascular lumen sustained cell viability and differentiation in an ≈ 16 cm^3 construct (Figure 2A–C).[36] The same research group also investigated the possibility of depositing perfusable vascular structures in a single-step process, bypassing the need for sacrificial bioinks to generate hollow channels.[37] Toward this end, the authors designed a three-layer coaxial nozzle to extrude hollow channels with lumen diameters up to 1 mm. While the first vascularization strategy focused on microvasculature formation, the second emphasized the formation of large blood vessels.[37] Regeneration of large tissues requires the presence of large vessels intimately connected with a diffuse capillary network and therefore a tradeoff between these two macrobioprinting approaches. Zhang and co-workers presented an alternative approach for the development of vascularized bones, focused on recapitulating the evolving signaling cascade that occurs in the native osteoblastic niche.[38] Extrusion-based bioprinting was used to produce BMP-2-functionalized poly(lactic acid) (PLA) into the honeycomb architecture of osteons, while stereolithography was used to form a vascular network out of gelatin methacrylate (GelMA) functionalized with vascular endothelial growth factor (VEGF). Creation of a central channel in the scaffold, mimicking the Haversian canal of osteons, allowed for scaffold perfusion and promoted maturation of bone and vascular tissue over the course of four weeks. This macrobioprinting strategy holds great promise for the regeneration of vascularized constructs but entails a complex combination of extrusion and stereolithography bioprinting, which might be challenging to adapt for high-throughput production of human-size constructs.[38] The study by Jang et al. is perhaps the most indicative of the advances made in bioprinting-based strategies for vascularized tissue repair

(Figure 2D–F). In this work, cardiac patches (≈25 mm^3 in volume) were fabricated via dual printing of heart tissue-derived ECM loaded with cardiac progenitor cells (CPCs) and MSCs.[39] Upon implantation in a rat myocar-dial infarction model, the fiber pattern derived from the use of extrusion-based bioprinting strongly promoted vasculogenesis within the implanted patch, with capillary formation differing from that observed in cardiac patches obtained with a conventional mold. This patterning allowed for spatial localization of CPCs and MSCs, with improved crosstalk between the two and ultimately the formation of stable blood vessels in the infarcted tissue.[39] This work highlights how complex tissues may be faithfully recapitulated via bioprinting both on a molecular level (angiogenic signaling) and on a physiological level (cardiac tissue function).[39]

Overall, future development in bioprinting-based vascular approaches will likely focus on three parallel aspects: (i) optimization of the CAD design and of the bioprinting technique to fabricate the full extent of vasculature (large vessels and micro-capillaries) at once, (ii) elucidation of the conditions required for endothelial/stem cells to maximize angiogenesis, and (iii) further improvement upon this last aspect via addition of tissue-specific ECM and/or growth factors to increase scaffold biomimicry.

Advances in bioprinting technology also positively impacted skin TE applications, where multiple attempts have been made on reproducing the multilayered structure of this tissue. The skin is the first barrier against external mechanical and biochemical agents, and is broadly composed of the epidermis, dermis, and hypodermis layers, each with its distinct composition and function.[40] Michael et al. mimicked this structure via laser-assisted bioprinting (LaBP) of collagen and Matriderm into three layers.[21] This approach sought to improve the clinical outcome of Matriderm implants, which often require the use of autologous skin grafts to complement the Matriderm layer.[41,42] The multilayer skin constructs showed full integration when implanted in the dorsal skin fold chamber of nude mice, but no comparison to single Matriderm implants was performed.[21] Jorcano and co-workers adapted the same system but opted for an extrusion-based bioprinting technique in order to fabricate larger skin constructs with higher throughput.[43] Mixing of cells, fibrin, and $CaCl_2$ (a coagulation agent for fibrinogen) occurred in a mixing nozzle immediately before extrusion. This choice allowed for higher extrusion rates with no detrimental effect on cell viability. Overall, the authors were able to generate a skin graft of ≈100 cm^2 in less than 35 min (including the 30 min required for fibrin gelation).[43] To further increase the speed of the skin bioprinting process, Skardal et al. adapted an in-house-built bioprinter to extrude skin grafts directly over a wound site.[44] In contrast to the two studies mentioned above, this method did not focus on recapitulating the complex structure of skin, but rather on developing a simple strategy that could be easily translated from bench to bedside.[44] Future studies will have to elucidate “how biomimetic” the skin constructs needs to be to achieve robust tissue formation in vivo, while being simple enough for high-throughput fabrication.

Other investigations have focused on tissues closely correlated with skin, namely, adipose tissue.[45] Pati et al. employed a highly biomimetic approach to bioprint custom-shaped adipose tissue, where human adipose tissue-derived mesenchymal stem cells (hASCs) were encapsulated in decellularized adipose tissue. Again, PCL was co-extruded to provide structural integrity to the resulting construct. Animal testing revealed minimal immune

response by the cell-laden constructs, which hold great promise in reconstructive surgery for the filling of patient-specific soft tissue defects.[45]

Macrobioprinting has also begun to find applicability in central nervous system (CNS) TE. Hsieh et al. engineered polyurethane (PU) nanoparticle dispersions as a carrier bioink for neural stem cell (NSC) delivery in CNS lesions.[46] Strikingly, partial recovery of CNS functions was observed in zebrafish models with traumatic brain injury and locomotive impairment although the scaffold design did not closely mimic the brain architecture.[46] Lozano et al. sought to address this last aspect in their work by recreating the structural complexity of the brain via extrusion-based bioprinting of gellan gum loaded with primary cortical neurons.[47] These highly biomimetic brain-like constructs mirrored the layered structure observed in the native cortex and were amenable to the encapsulation of layer-specific cortical neuron subtypes.[47]

However, further investigations are warranted to assess scaffold integration in vivo and recovery of cerebral functions. Extrusion-based bioprinting is particularly suitable for nerve TE due to the possibility of inducing cell/material alignment along a preferential axis, thus recapitulating the anatomy of neural networks. Along this line, Chen and co-workers developed a hybrid bioink composed of fibrin, thrombin, hyaluronic acid, and polyvinyl alcohol (HA/PVA) to encapsulate Schwann cells.[48] The anisotropic organization of the resulting 140 mm^3 construct induced preferential cell alignment and elongation of neuronal processes along the fibrin fiber, that is, along the extrusion axis.[48] Similarly, Owens et al. engineered nerve grafts hosting a central lumen to facilitate axon regrowth.[49] The grafts were tested in a rat sciatic nerve injury model, where the recovery of motor and sensory function was similar to that observed in animals treated with standard methods of nerve repair (autologous graft or collagen tube grafts control groups). Despite the limited dimension of the constructs, the positive findings warrant further investigation on the generation of nerve grafts of clinically relevant size.[49] It can be envisioned that future investigations in CNS TE will focus on further scaling up these systems, which can be technically challenging. In particular, larger constructs must maintain effective neuronal connections among the cells, a critical element in CNS physiology and functions.

In conclusion, macrobioprinting strategies have been successfully applied to a wide variety of tissues and organs, with restoration of physiological functions in vivo in several studies. Most of these research efforts focused on the musculoskeletal system, as shown in Table 1. Future investigations should build upon these promising findings to develop TE strategies for other organs in great demand, such as liver, lungs, and kidneys. Regardless of the target tissue, balancing the need for a complex scaffold (to faithfully mimic tissue anatomy) while developing a straightforward bioprinting strategy that can be easily translated from bench-to-bedside will remain a central challenge in macrobioprinting.

4. Microbioprinting for Tissue Modeling

As described in the previous section, bioprinting has become a widely used tool for the development, characterization, and study of complex organ tissues at the macroscale. Nevertheless, biological complexity is not specific to whole organs. Recent advances in 3D

printing technologies have provided such a high degree of control over bioprinting processes that they can be exploited to produce detailed features at the microscale. The possibility of fabricating microscopic features, such as wall thicknesses of 20 μm or pillars with a 32 × 32 μm cross section,[50,51] opens a new realm of opportunities to study the interactions of a single cell with its environment. As defined, microbioprinting is the application of bioprinting techniques at micro- and nanometer scale for the development of miniaturized devices for tissue modeling and interrogation of the cell microenvironment.

For example, stereolithography has been leveraged to produce cell-laden, porous hydrogel scaffolds with high-resolution features.[52,53] Lin et al. exploited this approach to process poly(ethylene glycol diacrylate) (PEGDA) into hollow cylindrical, hemispherical, cubical, and pyramidal structures with pore sizes down to 300 μm × 300 μm,[52] while Soman et al. used GelMA to fabricate complex geometries (spirals, pyramids, flower, and domes) with resolutions of 6–17 μm.[53] Both methods successfully use cell-laden inks, addressing a common challenge in high-energy systems such as stereolithography printers. In order to maximize cell viability, Lin et al. used visible light instead of UV-based curing,[52] while Soman et al. optimized the bioink composition for short exposure to UV.[53]

Similarly, direct-writing technologies have been used to produce solid scaffolds with complex geometries that promote nutrient diffusion by increasing the scaffold surface area. Tamayol et al. used alginate as a sacrificial template to physically entrap various prepolymer solutions into micropolymeric networks.[54] This method resulted in fibers with diameters ranging from 550 to 1000 μm. In contrast, Williams et al. used direct-writing bioprinting to form cellular cell-laden alginate spheroids with a diameter between 1500 and 2500 μm.[55] In both cases, increased surface area and compartmentalization of the cells promoted diffusion of nutrients and waste, reducing cell apoptosis.

The development of microbioprinting strategies to better interrogate cells within a physiological environment provided researchers with the tools to design and develop artificial cell niches. With each study, new bioprinting parameters are optimized to further recapitulate the cell microenvironment; however, the question remains, how much smaller and more complex does microbioprinting need to go? Furthermore, there is a need to correlate these cell niche findings to the complexity and specificity of organ systems.

Toward this end, microbioprinting approaches have been tailored for mechanistic studies on tissue vascularization. Diffusion requirements dictate the cells to be within a 100–200 μm radius of a blood vessel, the maximum distance for nutrients and oxygen diffusion in tissues.[56,57] Vasculature is thus a necessary step in TE and it is necessary to understand the basic biology behind angiogenesis and the formation of sustainable vascular networks. Microbioprinting allows the creation of complex microstructures, and it has been leveraged for: (i) the controlled deposition of cells/materials where tube formation and endothelialization are needed and for (ii) bioprinting vasculature-like microchannel configurations.

Capillaries can have diameters as small as 5 μm, small enough for a single red blood cell to squeeze through; controlled deposition in microbioprinting allows for the construction of

hollow tubular structures that mimic them. Most approaches accomplish this by exploiting fast-cross-linking techniques. The fast ionic reaction seen in the gelation of alginate using calcium ions has been widely used for this purpose.[58–60] Pataky et al. report the use of alginate droplet deposition for fast gelling producing microcapillaries with dimensions in the order of 2.3 μm on gelatin substrates and 4.4 μm on alginate films (Figure 3A–E).[58]

Simple deposition and extrusion technologies have been further optimized to produce tubes with microscopic diameters and wall thicknesses; these technologies include piezoelectric nozzles,[60] direct writing of guest–host hydrogels (GHost writing),[61] or freeform reversible embedding of suspended hydrogels (FRESH).[62] Hewes et al. reported the bioprinting of freestanding microvessels with endothelial cells embedded in a fibrin matrix using a single piezoelectric nozzle.[60] This approach can form 1–2 mm long tubes with 300 μm diameter in about 2 min.[60] Along the same line, the GHost writing technology developed by Burdick and co-workers allowed for bioprinting of shear-thinning hydrogel inks (the “guest”) directly into self-healing support (the “host”) hydrogels.[61] Using hyaluronic acid hydrogels, capillary-like filaments were printed in any direction in space, a characteristic that is not possible in air without supporting or sacrificial structures. Permeable vascular microchannels were obtained by bifurcating and rejoining structures of the guest ink, cross-linking the host network under UV light and then flushing the guest ink out, leaving behind open vascular patterns.[61] The FRESH approach, presented by the Feinberg group, uses a similar deposition technology (Figure 3F–H).[62] Here, a hydrogel is deposited within a second hydrogel support bath that maintains the intended structure during the print process and significantly improves print resolution. This method was used to successfully mimic a right coronary artery vascular tree with a hollow lumen and a wall thickness of <1 mm.[62]

Other novel 3D printing methods to develop permeable networks include coaxial microfluidic printing and microscale continuous optical bioprinting (mCOB).[57,59] The first technique uses a coaxial print head that produces a central flow of $CaCl_2$ solution surrounded by an annulus of sodium alginate, forming hollow tubes with diameters ranging from 0.5 to 2 mm.[59] Zhu et al. presented a digital light processing-based method to create prevascularized tissues: the mCOB method.[57] Here, different proportions of glycidal methacrylate–hyaluronic acid, GelMA, and photoinitiator LAP were UV-cross-linked with and without cells. Using mCOB, researchers printed an equivalent of a rat capillary network with features ranging from 5 to 50 μm.[57]

Sacrificial inks, such as Pluronic F-127, carbohydrate sugar glass, or agarose, have been used for the formation of embedded, permeable microchannels.[56,63,64] Kolesky et al. used Pluronic F-127 to form bifurcated networks encased in GelMA, yielding 3D microchannel arrays with diameters from 45 to 500 μm.[64] Permeability and endothelialization of the GelMA networks were further studied by flowing human umbilical vein-derived endothelial cells (HUVECs) or animal blood into the network.[64] Similarly, Miller et al. developed an approach to use carbohydrate sugar glass to fabricate complex vascular designs.[63] The sugar was extruded at high temperatures, producing filaments ranging from 150 to 750 μm that were then encased in a suspension of HUVECs and ECM prepolymer. The sugar was then dissolved using cell media, producing open channels where interfilament fusions

become intervessel junctions. This approach was used to produce multiscale architectures, such as single strands, interconnected Y-junctions, and curved filaments.[63] It is possible to print, via multiple different methodologies, patent vascular networks down to the micro- and nanoscale. The key question that needs to be addressed is how findings obtained in these networks correlate to in vivo data. Further studies must focus on the functionality of these vascular networks to sustain viable transport rates in a regenerating organ or tissue, rather than as isolated simple systems.

Microbioprinting has been further used to produce models of a variety of tissues including cardiac muscle, bone, cartilage, or skin. Microbioprinting has enabled researchers to study the effect of micropatterned cell deposition or micropatterned porous structures on the contractile response of cardiomyocytes to electrical stimulation.[65,66] For example, the Boland group fabricated micropatterned structures by depositing alginate/gelatin micro-droplets containing cardiomyocytes. Microbioprinting allowed for the formation of porous microstructures that would not have been possible using conventional manufacturing approaches, resulting in the production of viable cardiac muscle.[66]

As major load-bearing tissues, bone and cartilage rely on a delicate balance between mechanical properties and a porosity gradient to allow cell renewal and vascularization. Cartilage layers are gradually calcified and produce a continuous inter-phase into bone; thus, the recapitulation of these gradients is essential for cartilage tissue engineering. As such, Atala and co-workers reported a coculture printing method to mimic this stratification.[67] Electrospinning of PCL and inkjet bioprinting of chondrocyte⁄fibrinogen⁄collagen solutions were alternated to produce a layered cell-laden scaffold. These hybrid cartilage equivalents showed 80% cell viability, deposition of collagen and glycosaminoglycans, and enhanced mechanical properties compared to printed alginate or fibrin–collagen gels alone.[67]

As with cartilage, the possibility of fabricating multilayered scaffolds via bioprinting has been further leveraged in skin TE. The latest trends in dermal TE make extensive use of ink-jet deposition and laser-assisted bioprinting, which allow high control over the microstructures and spatiotemporal deposition of biomaterials and cells.[17,68] The overall approach to engineering skin relies on producing the skin's layered structure by using different hydrogels loaded with cells and/or growth factors. Novel approaches have used free-form deposition of layered collagen, keratinocytes, and fibro-blasts, cross-linked using nebulized sodium bicarbonate,[68] or bioprinting different biomaterials onto PDMS chips to fabricate in vitro skin models.[69] Although the layering approach has been widely used, the current variety of bioprinting technologies has optimized the layers down to the nanoscale. Novel systems include the Integrated Composite tissue/organ Building System (ICBS) presented by the Cho group[70] and the LaBP system reported by the Chichkov group.[22] Cho and co-workers presented the ICBS, a hybrid system with independent extrusion-based and inkjet-based modules, to position keratinocytes with spatial resolution in an epidermis–dermis scaffold.[70] The multihead ICBS can dispense PCL, sacrificial gelatin, and sequential layers of human primary dermal fibroblasts (HDFs) and epidermal keratinocytes (HEKs) suspended in collagen as the dermis and epidermis, respectively. The overall construct resulted in a very accurate layered profile of the dermis and epidermis, each with their cell population and ECM composition.[70] The LaBP system, based on laser-induced

forward transfer, was used by Koch et al. to arrange cells in 3D skin constructs (Figure 3I–K).[22] This system can accurately transfer and position cell suspension droplets as small as a few hundred femtoliters. Here, fibroblasts and keratinocytes embedded in collagen were transferred onto a Matriderm substrate to build a layered epidermis–dermis construct.[22]

Microbioprinting allows spatial and temporal control over the multiple components of a scaffold, making it an ideal technology for the development of gradients in multilayered tissues such as cartilage or skin. The impact of modifying the scaffolds at a microscale on the macroscopic mechanical functions of a tissue has been sparsely addressed. Future work in this area will require a to shift toward characterizing the functionality of the microscaffolds, and translating them to address patient needs.

As shown in Table 2, a significant portion of microbio-printed systems focuses on vascular or skin TE. This trend can be explained by the fact that current microbioprinting technologies are tailored for use with soft hydrogels (e.g., alginate, GelMA), which are suitable substrates for vasculature and skin formation. Future investigations in micro-bioprinting should focus on including synthetic materials to expand the realm of microbioprinting applications to other areas, namely, musculoskeletal TE. Microbioprinting approaches generally result in the fabrication of scaffolds with higher resolution compared to macrobioprinting approaches. Yet, the possibility to assemble microbioprinted constructs to create a large scaffold for organ regeneration is clinically unfeasible due to enormous amount of time required. Finally, it is imperative to correlate the basic biology obtained within macrobioprinted systems to in vivo data in order to validate these systems.

5. Macro- versus Microbioprinting

Here, we have highlighted the latest advances in bioprinting and emphasized how the field is moving into two distinctive lines of research. On the one hand, the efforts made toward the fabrication of large size scaffolds (>20 mm^3) suitable for clinical transplantation (macrobioprinting) and, on the other, the development of in vitro models able to capture the complexity of tissue organization down to the cellular level (microbioprinting). Based on the literature covered (Tables 1 and 2), Figure 4 presents a graphical comparison between macro- and microprinting, focusing on the types of tissues, the bioprinting technologies used, and the application for which the constructs were designed.

Strikingly, graphical comparison in Figure 5 shows how macrobioprinting strategies chiefly concentrated on musculoskeletal systems, while microbioprinting efforts focused on vasculature. This divergence can be ascribed by the bioprinting technologies employed in either field. Production of large constructs in a reasonable amount of time can be accomplished mainly via extrusion-based bioprinting, which at the same time can be leveraged to deposit bioinks with different biological and mechanical properties for load-bearing musculoskeletal TE, as extensively discussed in Section 2. Conversely, microbioprinting technologies rely mostly on the use of naturally derived hydrogels (e.g., alginate, collagen) and therefore have been mainly tailored for soft tissues, chiefly blood vessels and skin.

The fabrication of large tissues via macrobioprinting inevitably means larger volumes of materials needed and, correspondingly, technology that can effectively work with such quantities. As such, the vast majority (85%) of macrobioprinting studies rely on common extrusion technologies. The optimized devices, simple mechanics and biochemical reactions, and the fast dispensing, are the key characteristics why extrusion is the preferred technology in macrobioprinting. Other approaches, including variations of photolithography or laser-induced forward transfer, have been attempted to improve the spatiotemporal resolution of the resulting constructs, but the smaller volumes that can be managed and the longer print times are detrimental to cell survival and not feasible options for clinical use.

Microbioprinting has made consistent use of a wider range of technologies. Laser-assisted technologies or high-energy methods do achieve consistent micro-/nanofeatures, but the complexity of the systems and their effects on biological components remain a concern. About this aspect, it is worth highlighting that a growing body of TE literature uses 3D printing technologies (not strictly bioprinting) that provide high resolution but rely on high-energy systems (e.g., stereolithography, multiphoton cross-linking, or sintering) or on the use of aggressive chemicals. Both strategies increase the cross-link speed and specificity, produce highly detailed features, but result in poor cell viability. Accordingly, these strategies are usually leveraged to fabricate an acellular construct with high resolution that can then be seeded with the cells (Figure 5). Examples include collagen membranes with 1 μm features fabricated via multiphoton cross-linking,[51] tricalcium phosphate scaffolds with interconnected 300–1000 μm pore structures via sintering,[71] and pentaerythritol tetraacrylate (PETTA) processing via DLW (Figure 5).[72] The possibility to further develop these techniques for cell encapsulation would tremendously benefit microbioprinting, where a wider range of biomaterials (from natural to synthetic polymers) could be used to model a wider variety of tissues (from skin to bones) in vitro.

Microbioprinting strategies generally offer higher resolution than macrobioprinting strategies, but unfortunately cannot sustain the fabrication of human-size in a feasible amount of time. While several microbioprinted constructs can be theoretically assembled into a macroscopic construct, this choice would require a substantial amount of time, which (i) makes it clinically unfeasible and (ii) would negatively impact cell viability.

Regardless of the advances in each field, a critical point is the correlation between findings obtained at macro- and microscale. Microbioprinting focuses on in vitro modeling (89%), while macrobioprinting seeks solutions for in vivo tissue regeneration (55%). How do findings on the microscale inform scaffold design at the macroscale? The questions that can be currently addressed with microbioprinting remain anchored in basic biology, mostly understanding how cells interact with their microenvironment either from a general standpoint (cell niche studies) or from a tissue-specific approach (tissue cells on specialized scaffolds). On the other hand, macrobioprinting is limited to general design questions, but these can be assayed under physiological conditions in living specimens. Future investigations should elucidate whether, for a given tissue, the different processing used in macro- and microbioprinting application affect cell phenotype to such extent that biological findings obtained cannot be reconciled.

6. Conclusions

Macrobioprinting strategies hold great promise for the regeneration of large tissue due to the possibility to fabricate custom-shaped constructs with anatomically relevant properties. On the other end of the spectrum, microbioprinting strategies provide mechanistic notions on tissue formation.

Fabrication of functional organ surrogates requires both the recapitulation of the complex cell/ECM pattern observed in the native organ as well as creation of a mechanically stable backbone able to provide structural support to the overall constructs.

In order to mimic the complex cell/ECM pattern observed in the native organ while fabricating a mechanically stable construct, most microbioprinting approaches leverage the versatility of extrusion-based bioprinting to deposit different materials simultaneously, usually a synthetic polymer responsible for mechanical properties and a naturally derived poly mer for enhanced biological activity. It can be envisioned that coprinting of multiple bioinks with complementary properties (synthetic and natural materials) will remain the main strategy to address the requirements of structural integrity and biomimicry. Finally, the use of physiologically relevant bioinks, that is, natural biopolymers containing tissue-specific decellularized ECM or growth factors, is expected to remain the main approach to enhance scaffold biomimicry.

Microbioprinting strategies provide high-resolution tissue mimics to model specific aspects of the tissue microenvironment. Yet, these technologies mainly use soft materials and therefore found marginal applicability in load-bearing applications. Future investigations should address this limitation by expanding current microbioprinting technologies to the use of harder polymers, namely, synthetic materials and ceramics.

Ultimately, significant advances in TE and regenerative medi cine are likely to occur when findings obtained on the microscale via microbioprinting will serve as design criteria for macrobioprinting scaffolds of clinically relevant size.

Acknowledgements

M.S. and J.N. contributed equally to this work. This research was supported by the Maryland Stem Cell Research Fund (MSCRF) Research Grant (No. 4300811), and the National Institute of Biomedical Imaging and Bioengineering / National Institutes of Health (NIBIB/NIH) Center for Engineering Complex Tissues (P41 EB023833). M.S. acknowledges support from the MSCRF Postdoctoral Fellowship Program, while J.N. acknowledges support from the Fulbright Scholars Program. The authors thank Justine R. Yu for assistance with manuscript preparation.

Biographies

Marco Santoro works as a postdoctoral associate in bio-engineering at the University of Maryland, College Park. He received in Ph.D. in chemical and biomolecular engineering from Rice University (Houston, TX) in 2016. His research focuses on angiogenesis in 3D-printed cocultures for the fabrication of vascularized scaffolds via bioprinting. Additionally, he is investigating the use of two-photon stereolithography to study heterotypic cell–cell interaction on a chip.

Javier Navarro received his master's degree in mechanical engineering from Universidad de Los Andes (Bogota, Colombia) in 2012. He is currently a Ph.D. candidate in bioengineering under the supervision of Dr. John P. Fisher at the University of Maryland, College Park. His research project is focused on the understanding of cellular cues that drive formation of gradients or layers in tissues, and the development of stratified regenerative scaffolds for the treatment of facial burn wounds. He is also interested in 3D printing of biomolecules such as keratin and dermal extracellular matrix.

John P. Fisher is the Fischell family distinguished professor and chair of the department of bioengineering at the University of Maryland, College Park. He received his Ph.D. in chemical engineering from Rice University (Houston, TX) in 2003. His research is focused on the design and fabrication of scaffolds for tissue engineering applications by combining biomaterials with cells and/or growth factors. He is also interested in the synthesis of novel hydrolytically degradable and implantable polymers for cell and drug delivery.

References

[1]. Zhang YS, Yue K, Aleman J, Mollazadeh-Moghaddam K, Bakht SM, Yang J, Jia W, Dell'Erba V, Assawes P, Shin SR, Dokmeci MR, Oklu R, Khademhosseini A, Ann. Biomed. Eng 2017, 45, 148. [PubMed: 27126775]

[2]. Ozbolat IT, Peng W, Ozbolat V, Drug Discovery Today 2016, 21, 1257. [PubMed: 27086009]

[3]. V Murphy S, Atala A, Nat. Biotechnol 2014, 32, 773. [PubMed: 25093879]

[4]. Derby B, Science 2012, 338, 921. [PubMed: 23161993]

[5]. Knowlton S, Yenilmez B, Tasoglu S, Trends Biotechnol. 2016, 34, 685. [PubMed: 27424152]

[6]. Albritton JL, Miller JS, Dis. Model. Mech 2017, 10, 3. [PubMed: 28067628]

[7]. Peng W, Unutmaz D, Ozbolat IT, Trends Biotechnol. 2016, 34, 722. [PubMed: 27296078]

[8]. Memic A, Navaei A, Mirani B, Cordova JAV, Aldhahri M, Dolatshahi-Pirouz A, Akbari M, Nikkhah M, Biotechnol. Lett 2017, 39, 1279. [PubMed: 28550360]

[9]. Sohn E, Sohn E-H, FASEB J. 2017, 31, 981.6.

[10]. Pedde RD, Mirani B, Navaei A, Styan T, Wong S, Mehrali M, Thakur A, Mohtaram NK, Bayati A, Dolatshahi-Pirouz A, Nikkhah M, Willerth SM, Akbari M, Adv. Mater 2017, 29, 1606061.

[11]. Mandrycky C, Wang Z, Kim K, Kim DH, Biotechnol. Adv 2016, 34, 422. [PubMed: 26724184]

[12]. Gauvin R, Chen YC, Lee JW, Soman P, Zorlutuna P, Nichol JW, Bae H, Chen S, Khademhosseini A, Biomaterials 2012, 33, 3824. [PubMed: 22365811]

[13]. Jose RR, Rodriguez MJ, Dixon TA, Omenetto F, Kaplan DL, ACS Biomater. Sci. Eng 2016, 2, 1662.

[14]. Ji S, Guvendiren M, Front. Bioeng. Biotechnol 2017, 5, 23. [PubMed: 28424770]

[15]. Hospodiuk M, Dey M, Sosnoski D, Ozbolat IT, Biotechnol. Adv 2017, 35, 217. [PubMed: 28057483]

[16]. Shafiee A, Atala A, Trends Mol. Med 2016, 22, 254. [PubMed: 26856235]
[17]. Singh D, Singh D, Han SS, Polymers 2016, 8, 19.
[18]. Mosadegh B, Xiong G, Dunham S, Min JK, Biomed. Mater 2015, 10, 34002.
[19]. Datta P, Ayan B, Ozbolat IT, Acta Biomater. 2017, 51, 1. [PubMed: 28087487]
[20]. Daly AC, Freeman FE, Gonzalez-Fernandez T, Critchley SE, Nulty J, Kelly DJ, Adv. Healthcare Mater 2017, 6, 1700298.
[21]. Michael S, Sorg H, Peck CT, Koch L, Deiwick A, Chichkov B, Vogt PM, Reimers K, PLoS One 2013, 8, e57741. [PubMed: 23469227]
[22]. Koch L, Deiwick A, Schlie S, Michael S, Gruene M, Coger V, Zychlinski D, Schambach A, Reimers K, Vogt PM, Chichkov B, Biotechnol. Bioeng 2012, 109, 1855. [PubMed: 22328297]
[23]. Gao G, Cui X, Biotechnol. Lett 2016, 38, 203. [PubMed: 26466597]
[24]. Daly AC, Cunniffe GM, Sathy BN, Jeon O, Alsberg E, Kelly DJ, Adv. Healthcare Mater 2016, 5, 2353.
[25]. Shim J, Lee J, Kim J, Cho D, J. Micromech. Microeng 2012, 22, 85014.
[26]. Shim J-H, Jang K-M, Hahn SK, Park JY, Jung H, Oh K, Park KM, Yeom J, Park SH, Kim SW, Wang JH, Kim K, Cho D-W, Biofabrication 2016, 8, 14102.
[27]. Gurkan UA, El Assal R, Yildiz SE, Sung Y, Trachtenberg AJ, Kuo WP, Demirci U, Mol. Pharm 2014, 11, 2151. [PubMed: 24495169]
[28]. Lee CH, Rodeo SA, Fortier LA, Lu C, Erisken C, Mao JJ, Sci. Transl. Med 2014, 6, 266ra171.
[29]. Levato R, Visser J, A Planell J, Engel E, Malda J, Mateos-Timoneda MA, Biofabrication 2014, 6, 35020.
[30]. Kim YB, Lee H, Yang GH, Choi CH, Lee DW, Hwang H, Jung WK, Yoon H, Kim GH, Colloid Interface Sci J. 2016, 461, 359.
[31]. Kang H-W, Lee SJ, Ko IK, Kengla C, Yoo JJ, Atala A, Nat. Biotechnol 2016, 34, 312. [PubMed: 26878319]
[32]. Bae H, Puranik AS, Gauvin R, Edalat F, Carrillo-Conde B, Peppas NA, Khademhosseini A, Sci. Transl. Med 2012, 4, 160ps23.
[33]. Kim JJ, Hou L, Huang NF, Acta Biomater. 2016, 41, 17. [PubMed: 27262741]
[34]. Wang Y, Wan C, Deng L, Liu X, Cao X, Gilbert SR, Bouxsein ML, Faugere MC, Guldberg RE, Gerstenfeld LC, Haase VH, Johnson RS, Schipani E, Clemens TL, J. Clin. Invest 2007, 117, 1616. [PubMed: 17549257]
[35]. Kusumbe AP, Ramasamy SK, Adams RH, Nature 2014, 507, 323. [PubMed: 24646994]
[36]. Byambaa B, Annabi N, Yue K, Trujillo-de Santiago G, Alvarez MM, Jia W, Kazemzadeh-Narbat M, Shin SR, Tamayol A, Khademhosseini A, Adv. Healthcare Mater 2017, 6, 1700015.
[37]. Jia W, Gungor-Ozkerim PS, Zhang YS, Yue K, Zhu K, Liu W, Pi Q, Byambaa B, Dokmeci MR, Shin SR, Khademhosseini A, Biomaterials 2016, 106, 58. [PubMed: 27552316]
[38]. Cui H, Zhu W, Nowicki M, Zhou X, Khademhosseini A, Zhang LG, Adv. Healthcare Mater 2016, 5, 2174.
[39]. Jang J, Park HJ, Kim SW, Kim H, Park JY, Na SJ, Kim HJ, Park MN, Choi SH, Park SH, Kim SW, Kwon SM, Kim PJ, Cho DW, Biomaterials 2017, 112, 264. [PubMed: 27770630]
[40]. Markeson D, Pleat JM, Sharpe JR, Harris AL, Seifalian AM, Watt SM, Tissue Eng J. Regener. Med 2015, 9, 649.
[41]. Singer AJ, Clark RA, Engl N. J. Med 1999, 341, 738.
[42]. Supp DM, Boyce ST, Clin. Dermatol 2005, 23, 403. [PubMed: 16023936]
[43]. Cubo N, Garcia M, del Cañizo JF, Velasco D, Jorcano JL, Biofabrication 2016, 9, 15006.
[44]. Skardal A, Mack D, Kapetanovic E, Atala A, Jackson JD, Yoo J, Soker S, Stem Cells Transl. Med 2012, 1, 792. [PubMed: 23197691]
[45]. Pati F, Ha DH, Jang J, Han HH, Rhie JW, Cho DW, Biomaterials 2015, 62, 164. [PubMed: 26056727]
[46]. Hsieh FY, Lin HH, Hsu SH, Biomaterials 2015, 71, 48. [PubMed: 26318816]
[47]. Lozano R, Stevens L, Thompson BC, Gilmore KJ, Gorkin R, Stewart EM, in het Panhuis M, Romero-Ortega M, Wallace GG, Biomaterials 2015, 67, 264. [PubMed: 26231917]

[48]. England S, Rajaram A, Schreyer DJ, Chen X, Bioprinting 2017, 5, 1.

[49]. Owens CM, Marga F, Forgacs G, Heesch CM, Biofabrication 2013, 5, 1.

[50]. Koroleva A, Gittard S, Schlie S, Deiwick A, Jockenhoevel S, Chichkov B, Biofabrication 2012, 4, 15001.

[51]. Bell A, Kofron M, Nistor V, Biofabrication 2015, 7, 35007.

[52]. Lin H, Zhang D, Alexander PG, Yang G, Tan J, Cheng AWM, Tuan RS, Biomaterials 2013, 34, 331. [PubMed: 23092861]

[53]. Soman P, Chung PH, Zhang AP, Chen S, Biotechnol. Bioeng 2013, 110, 3038. [PubMed: 23686741]

[54]. Tamayol A, Najafabadi AH, Aliakbarian B, Arab-Tehrany E, Akbari M, Annabi N, Juncker D, Khademhosseini A, Adv. Health-care Mater 2015, 4, 2146.

[55]. Williams SK, Touroo JS, Church KH, Hoying JB, Biores. Open Access 2013, 2, 448. [PubMed: 24380055]

[56]. Bertassoni LE, Cecconi M, Manoharan V, Nikkhah M, Hjortnaes J, Cristino AL, Barabaschi G, Demarchi D, Dokmeci MR, Yang Y, Khademhosseini A, Lab Chip 2014, 14, 2202. [PubMed: 24860845]

[57]. Zhu W, Qu X, Zhu J, Ma X, Patel S, Liu J, Wang P, Lai CSE, Gou M, Xu Y, Zhang K, Chen S, Biomaterials 2017, 124, 106. [PubMed: 28192772]

[58]. Pataky K, Braschler T, Negro A, Renaud P, Lutolf MP, Brugger J, Adv. Mater 2012, 24, 391. [PubMed: 22161949]

[59]. Attalla R, Ling C, Selvaganapathy P, Biomed. Microdevices 2016, 18, 17. [PubMed: 26842949]

[60]. Hewes S, Wong AD, Searson PC, Bioprinting 2016, 7, 14.

[61]. Highley CB, Rodell CB, Burdick JA, Adv. Mater 2015, 27, 5075. [PubMed: 26177925]

[62]. Hinton TJ, Jallerat Q, Palchesko RN, Park JH, Grodzicki MS, Shue H-J, Ramadan MH, Hudson AR, Feinberg AW, Sci. Adv 2015, 1, e1500758. [PubMed: 26601312]

[63]. Miller JS, Stevens KR, Yang MT, Baker BM, Nguyen D-HT, Cohen DM, Toro E, Chen AA, Galie PA, Yu X, Chaturvedi R, Bhatia SN, Chen CS, Nat. Mater 2012, 11, 768. [PubMed: 22751181]

[64]. Kolesky DB, Truby RL, Gladman AS, Busbee TA, Homan KA, Lewis JA, Adv. Mater 2014, 26, 3124. [PubMed: 24550124]

[65]. Adams SD, Ashok A, Kanwar RK, Kanwar JR, Kouzani AZ, Bioprinting 2017, 6, 18.

[66]. Xu T, Baicu C, Aho M, Zile M, Boland T, Biofabrication 2009, 1, 35001.

[67]. Xu T, Binder KW, Albanna MZ, Dice D, Zhao W, Yoo JJ, Atala A, Biofabrication 2012, 5, 15001.

[68]. Lee V, Singh G, Trasatti JP, Bjornsson C, Xu X, Tran TN, Yoo S-S, Dai G, Karande P, Tissue Eng., Part C 2014, 20, 473.

[69]. Lee W, Debasitis JC, Lee VK, Lee JH, Fischer K, Edminster K, Park JK, Yoo SS, Biomaterials 2009, 30, 1587. [PubMed: 19108884]

[70]. Kim BS, Lee J-S, Gao G, Cho D-W, Biofabrication 2017, 9, 25034.

[71]. Tarafder S, Davies NM, Bandyopadhyay A, Bose S, Biomater. Sci 2013, 1, 1250. [PubMed: 24729867]

[72]. Tarafder S, Balla VK, Davies NM, Bandyopadhyay A, Bose S, Tissue Eng J. Regener. Med 2013, 7, 631.

[73]. Greiner AM, Jäckel M, Scheiwe AC, Stamow DR, Autenrieth TJ, Lahann J, Franz CM, Bastmeyer M, Biomaterials 2014, 35, 611. [PubMed: 24140047]

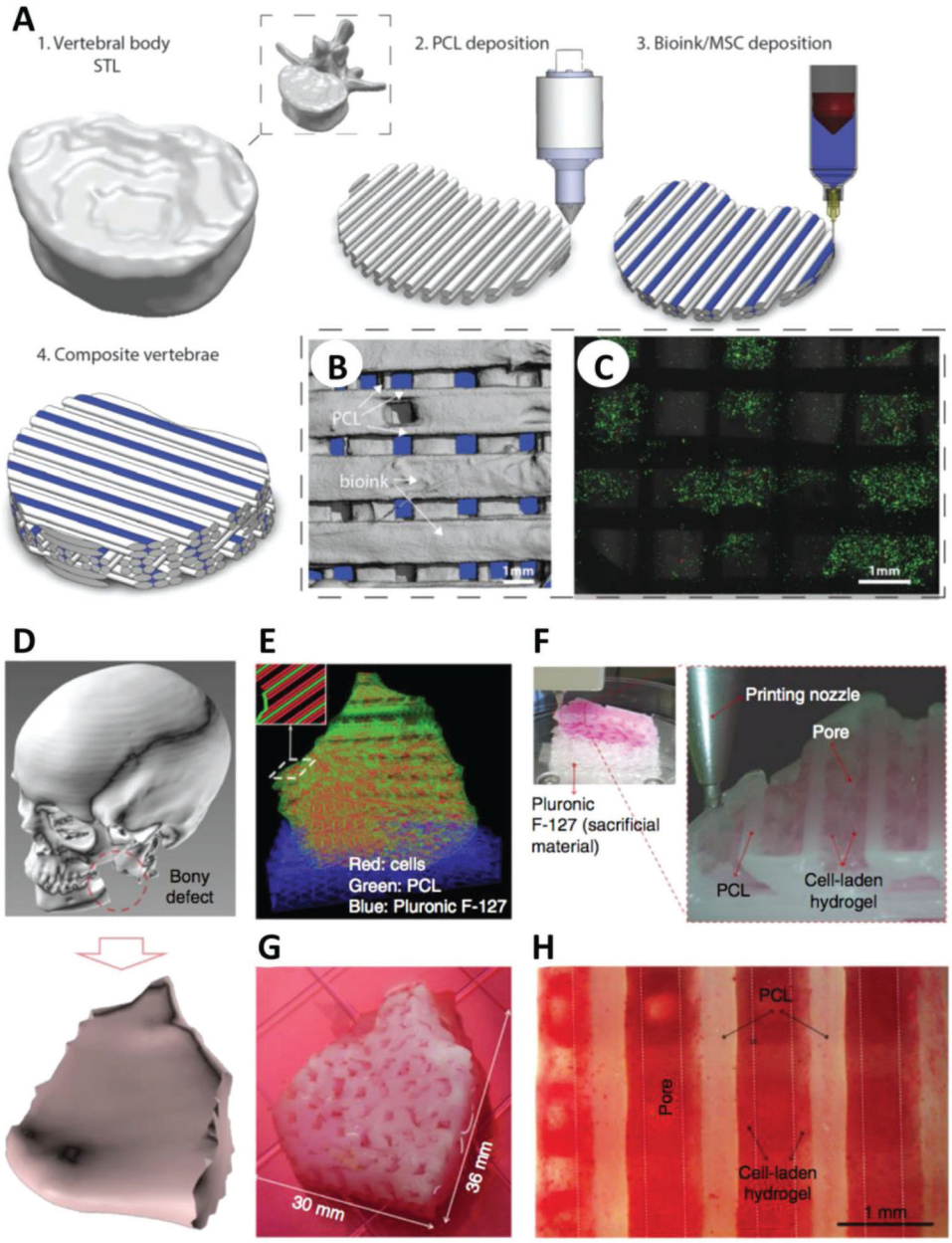

Figure 1.

Macrobioprinting of human vertebrae and mandible. A) The geometry of a human vertebra was scanned and bioprinted via extrusion of PCL and MSC-laden alginate/GelMA in an orthogonal fashion. B,C) Microcomputed tomography (B) and live/dead imaging (C) of cells demonstrated the distribution of materials/cells (live cells in green in (C)) within the macrobioprinted vertebrae. A–C) Adapted with permission.[24] Copyright 2016, Wiley-VCH. D–G) Patient data of a mandible defect (D) were used to develop a CAD model for a scaffold (E), which was then bioprinted by depositing alternate fibers of PCL (green), Pluronic F-127 (blue) and cell-laden hydrogel (red) (F,G). H) Alizarin Red staining confirmed the osteogenic differentiation of stem cells in the printed construct. D–H)

Adapted by permission.[31] Copyright 2016, Macmillan Publishers Ltd. Scale bars in (B), (C), and (H) are 1 mm.

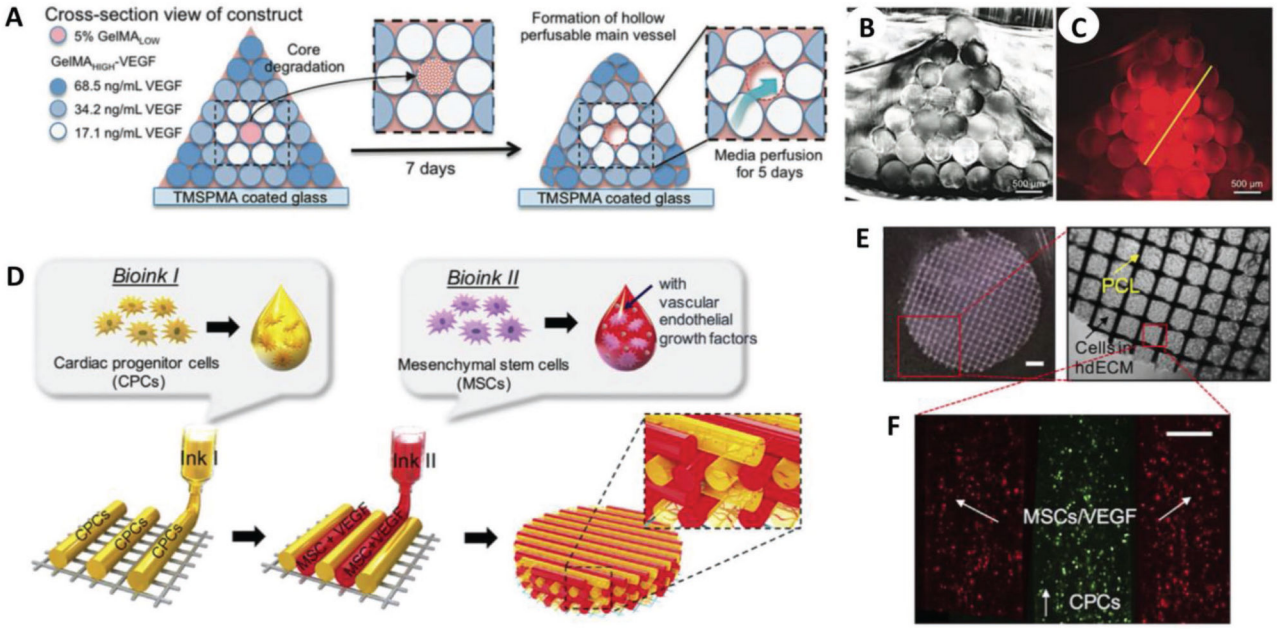

Figure 2.

Macrobioprinting of vascularized bone niche and cardiac patch. A) Vascularized bone constructs were fabricated as pyramidal constructs hosting a perfusable vascular lumen lined with HUVECs (pink) and array of hMSCs-laden VEGF-functionalized GelMA fibers with different mechanical strengths. B) Imaging of cross section of the resulting scaffold. C) Imaging of cross-sectional fluorescence gradient to show different chemical functionalization of bioprinted fibers. Scale bars in (B) and (C) are 500 μm. A–C) Adapted with permission.[36] Copyright 2017, Wiley-VCH. D) Bioprinting design of prevascularized cardiac patches, E) where a PCL layer provides structural support for F) two cell-laden bioinks. Scale bar in (E) (left) is 1 mm, while the scale bar in (F) is 200 μm. D–F) Adapted with permission.[39] Copyright 2017, Elsevier.

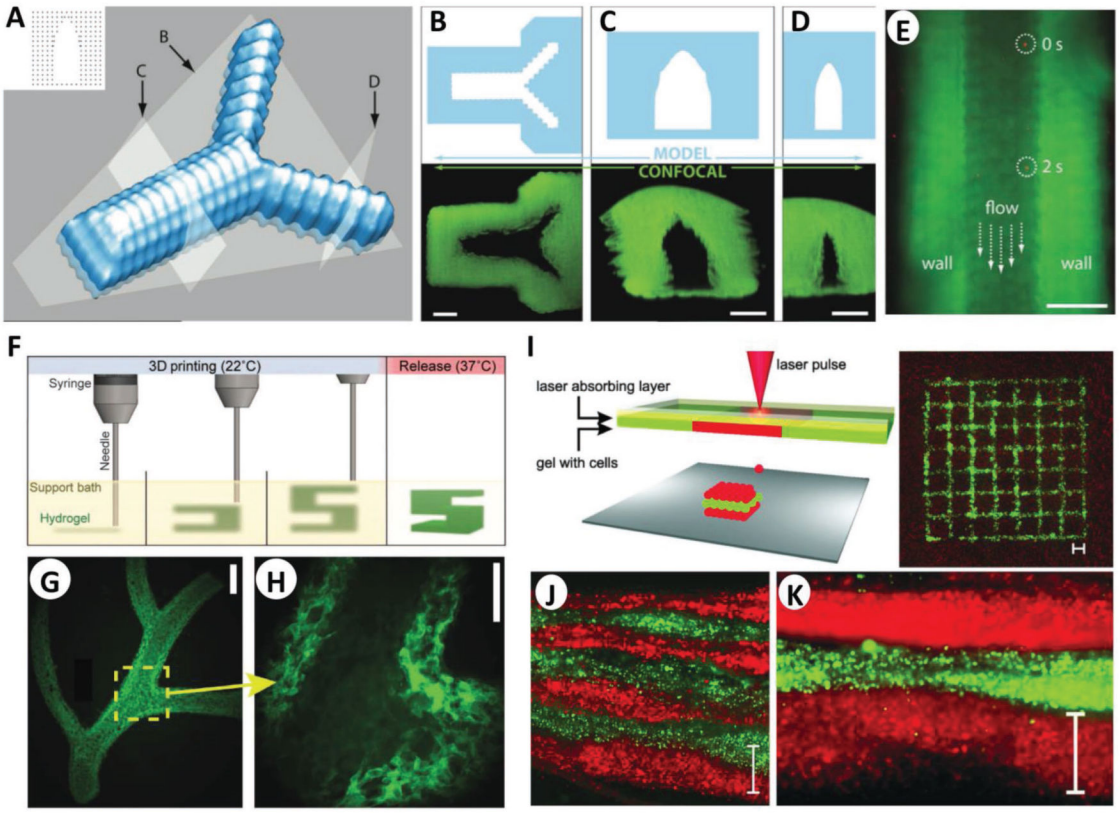

Figure 3.

Microbioprinting of vasculature and skin models. A) Rendering of the microvasculature model developed by Pataky et al. B–D) Slices of the model and confocal images according to the slicing planes labeled in (A). E) Composite image showing perfusion of the alginate microchannel with fluorescent beads flowing at 0 and 2 s. The scale bars in (B)–(E) represent 200 μm. A–E) Adapted with permission.[58] Copyright 2012, Wiley-VCH. F) Schematic of the FRESH process developed by Feinberg and co-workers, where a hydrogel (green) is extruded and cross-linked in a gelatin slurry (yellow). Upon completion, the system is heated to 37 °C to melt the gelatin and release the scaffold. G) Example of arterial trees printed in fluorescent alginate (green) via the FRESH method, H) where a stable lumen was formed with and defined vessel wall <1 mm thick. Scale bars are 2.5 and 1 mm in (G) and (H), respectively. F–H) Adapted with permission.[62] Copyright 2015, American Association for the Advancement of Science. I) Schematic of the microbioprinting setup used by Koch et al. (left), where the pressure of a laser-induced vapor bubble propels a cell-laden hydrogel and yields a micropatterned grid structure (right) of fibroblasts (green) and keratinocytes (red). J) Histology image showing seven alternating layers of red and green keratinocytes, where each colored layer consists of four microbioprinted sublayers. Scale bar is 500 μm in (I)–(K). I–K) Adapted with permission.[22] Copyright 2012, Wiley-VCH.

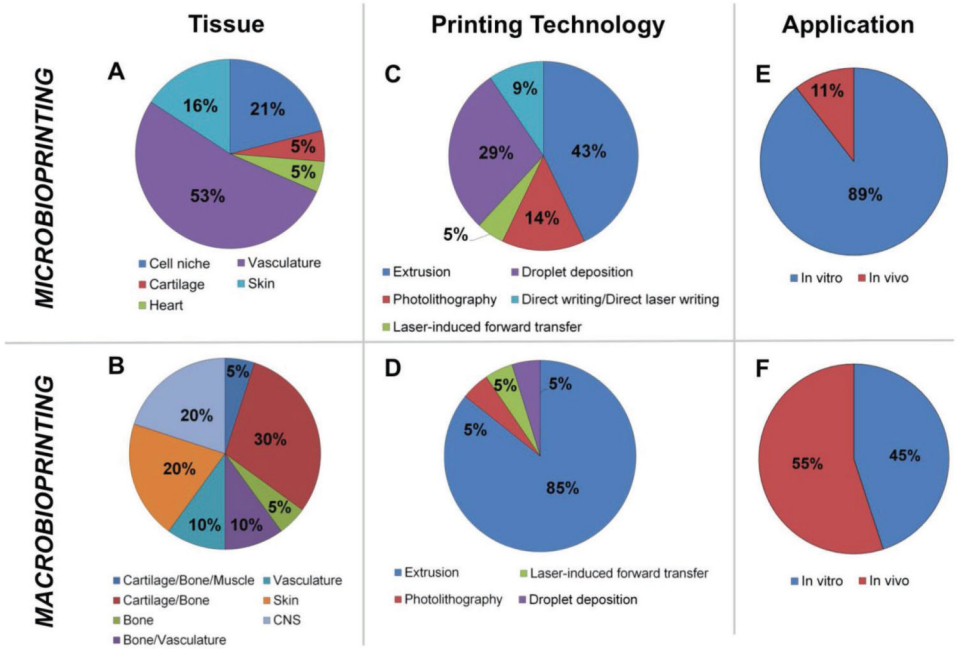

Figure 4.

Macro- versus microbioprinting. Graphical comparison of the findings in macro- and microbioprinting presented in Sections 2 and 3. Quantitative comparison focused on: A,B) the type of tissues that was bioprinted, C,D) the bioprinting technologies used, and E,F) the application stage in which the constructs were used. A,B) Microbioprinting approaches make use of soft hydrogel as bioink, limiting therefore their applicability to soft-tissue modeling, particularly vasculature and skin. Conversely, macrobioprinting strategies have been mainly leveraged for musculoskeletal TE applications, due to the possibility of combining materials with a wide range of mechanical properties. C,D) A wide range of technologies has been used for tissue modeling via microbioprinting, while macrobioprinting vastly relies on extrusion-based bioprinting to fabricate large constructs in a short amount of time. E,F) As per our definition, microbioprinting strategies focus on the development of highly detailed tissue models, understanding the interaction between cells and their tissue-specific niches, and are thus mainly applied for in vitro studies (89%). A small portion of these studies have been extended into in vivo stages (11%),[57,67] to further assess microprinted features in living environments. The aim of macrobioprinting approaches is to develop viable tissue constructs and the majority has already reached in vivo testing stage (55%) after initial in vitro testing. Despite 45% of applications having not been tested in vivo, they are purposely developed for tissue reconstruction.

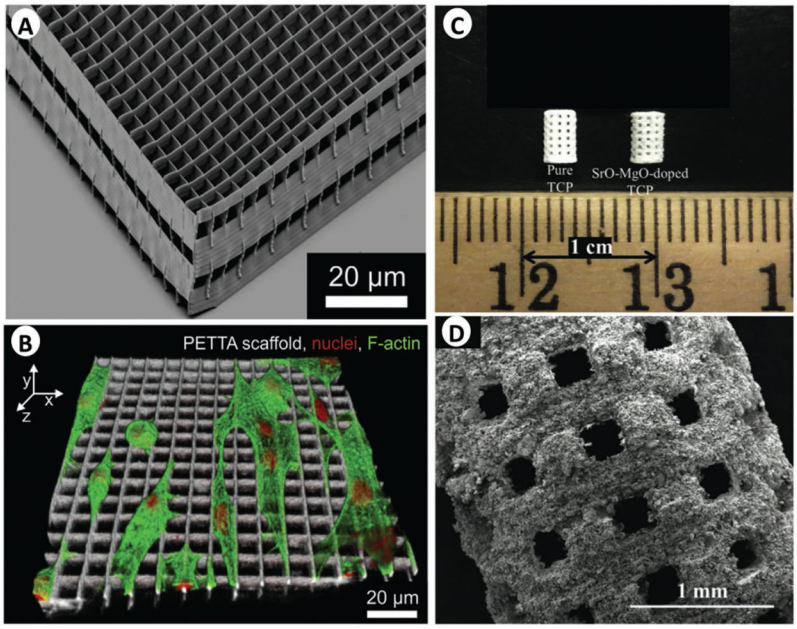

Figure 5.

Acellular micro-3D printing. A,B) Scanning electron microscopy images of pentaerythritol tetraacrylate (PETTA) processed by direct laser writing (A), which was developed by Greiner et al. to investigate cell invasion and morphology (nuclei in red, F-actin in green, and scaffold in white) (B). A,B) Adapted with permission.[72] Copyright 2014, Elsevier. C) Image of microwave sintered tricalcium phosphate (TCP) and Sr-Mg-doped TCP scaffolds, and D) an SEM image of the TCP scaffold. C,D) Adapted with permission.[71] Copyright 2013, The Royal Society of Chemistry.

Table 1.

Macrobioprinting strategies for large tissue regeneration.

Tissue	Printing technology	Bioink formulation	Scaffold size/ volume	Application			Ref.
				In vitro	In vivo	Clinical study	
Cartilage/bone	Extrusion	PCL and MSC-laden alginate/GelMA	10 mm Ø × 6 mm h 471 mm^3	✓	✓		[24]
Cartilage/bone	Extrusion	PCL, chondrocyte-laden alginate, and osteoblastladen alginate	270 × 130 × 100 mm 3.51×10^6 mm^3	✓			[25]
Cartilage/bone	Extrusion	PCL, MSC/TGF-β3-laden HA, and MSC/BMP-2-laden collagen	5 mm Ø × 5 mm h 98 mm^3		✓		[26]
Cartilage/bone	Microvalve printing	MSC-laden GelMA-loaded with TGF-β1 or BMP-2	10 × 10 × 1 mm 100 mm^3	✓			[27]
Cartilage/bone	Extrusion	PCL/PLGA loaded with TGF-β3 and/or CTGF	15 × 30 × 5 mm 2.25×10^3 mm^3	✓	✓		[28]
Cartilage/bone	Extrusion	MSC-laden PLA microcarriers in GelMA/gellan gum	16 mm Ø × 10 mm h 2.01×10^3 mm^3	✓			[29]
Bone	Extrusion	PCL and MG63-laden alginate	15 × 15 × 1.35 mm 304 mm^3	✓			[30]
Cartilage/bone/muscle	Extrusion	Variable, PCL and cellladen gelatin/fibrinogen/HA	Variable, largest 30 × 30 × 15 mm 1.35×10^3 mm^3		✓		[31]
Bone/vasculature	Extrusion	MSCs/HUVECs in VEGFconjugated GelMA	30 mm thick pyramids 16.5×10^3 mm^3	✓			[36]
Bone/vasculature	Extrusion	GelMA/alginate with cells	8 × 9 × 2.5 mm 180 mm^3	✓			[37]
Vasculature	Extrusion/SLA	MSCs/HUVECs in VEGFor BMP-2-conjugated GelMA and PLA	9 mm Ø × 4 mm h 254 mm^3	✓			[38]
Vasculature	Extrusion	Cardiac progenitor cells and/or MSCs in human ECM with VEGF	8 mm Ø × 0.5 mm h 25 mm^3	✓	✓		[39]
Skin	Laser-assisted bioprinting	Keratinocytes/fibroblasts in collagen and Matriderm	6 mm Ø × 1 mm h 28 mm^3	✓	✓		[21]
Skin	Extrusion	Keratinocytes/fibroblasts in fibrin	100 × 100 × 1 mm 10^4 mm^3	✓	✓		[43]
Skin	Extrusion	Stem cells in fibrin/collagen	20 × 20 × 0.2 mm 80 mm^3	✓	✓		[44]
Skin	Extrusion	hASCs in adipose tissuederived ECM and PCL	10 mm Ø × 5 mm h 393 mm^3	✓	✓		[45]
CNS	Extrusion	Neural stem cells in PU nanoparticles	15 × 15 × 0.2 mm	✓	✓		[46]

Tissue	Printing technology	Bioink formulation	Scaffold size/ volume	Application			Ref.
				In vitro	In vivo	Clinical study	
			45 mm^3				
CNS	Extrusion	Neurons in gellan gum	10 mm Ø × 5 mm h 393 mm^3	✓			[47]
CNS	Extrusion	Schwann cells in fibrin/HA/PVA	14 × 5 × 2 mm 140 mm^3	✓			[48]
CNS	Extrusion	Schwann cells/MSCs in agarose	2 mm Ø × 10 mm h a31 mm^3	✓	✓		[49]

Table 2.

Microbioprinting strategies for tissue modeling.

Tissue	Printing technology	Bioink formulation	Microprinted features	Application			Ref.
				In vitro	In vivo	Clinical study	
Cell niche	Visible light projection stereolithography	hASCs in a PEGDA	Cylinders, cubes, hemispheres, and pyramids with 300 × 300 μm pores	✓			[52]
Cell niche	UV photolithography	Fibroblasts and MSCs in GelMA	100–250 μm thick scaffolds with 6–17 μm resolution	✓			[53]
Cell niche	Wet-spinning, direct writing	Alginate template for gelatin, PVA, agarose, PEGDA, cell-laden GelMA	Fibers with 550–1000 μm Ø	✓			[54]
Cell niche	Direct writing, droplet deposition	Human stromal vascular cells in alginate	Spheroids with 1500–2500 μm Ø	✓			[55]
Cartilage	Inkjet bioprinting, electrospinning	PCL and chondrocyte-laden fibrinogen/ collagen	100–300 μm thick layers	✓	✓		[67]
Heart	Microdroplet deposition	Alginate/gelatin solution containing cardiomyocytes	Droplets produce hollow shells (pores) with 25 μm Ø	✓			[66]
Vasculature	Droplet deposition	Fibroblast-laden alginate deposition into gelatin	Capillaries with 2.3–4.4 μm Ø	✓			[58]
Vasculature	Extrusion	HUVEC-laden alginate tubes	Hollow tubes with 500–2000 μm Ø	✓			[59]
Vasculature	Piezoelectric inkjet deposition	HUVEC-laden alginate/fibrin	Tubes with 300 μm Ø, 1–2 mm height	✓			[60]
Vasculature	Extrusion using “Ghost” writing technology	Conjugated adamantane or β-cyclodextrin to HA	Permeable channels with 200 μm Ø	✓			[61]
Vasculature	Extrusion using FRESH technology	Myoblast-laden alginate in gelatin slurry	<1 mm features	✓			[62]
Vasculature	UV-DLP, microscale continuous optical bioprinting	HUVEC/stem-cell-laden GelMA	Capillary networks with 50–250 μm Ø gradient and 5–50 μm features	✓	✓		[57]
Vasculature	Extrusion	Pluronic F-127, cell-laden GelMA	Microchannels with 45–500 μm Ø	✓			[64]
Vasculature	Extrusion	Cell-laden GelMA, PEGDMA, SPELA, or PEGDA in agarose	Microchannels with 100–1000 μm Ø	✓			[56]
Vasculature	Extrusion	Carbohydrate glass, HUVEC-laden ECM-like hydrogels	Filaments with 150–750 μm Ø	✓			[63]
Vasculature	Extrusion	PLA, poly(L-lysine), and gelatin coating	500 μm Ø channels, 200 μm Ø pores	✓			[73]
Skin	Extrusion	Fibroblast- or keratinocyte-laden collagen	100–1400 μm thick layers, 30 μm thick cell-laden layers	✓			[68,69]
Skin	Extrusion, inkjet-bioprinting	PCL, gelatin, and fibroblast- or keratinocyte-laden collagen	PCL of 22 mm Ø, 400 μm height, and 100 μm pore Ø. 97 μm thick gelatin layers	✓			[70]
Skin	Laser-assisted bioprinting, based on laser-induced forward transfer	Cell-laden collagen or alginate loaded with human blood plasma	10 × 10 × 2 mm scaffold made of nanodroplets in the 0.1–1 nL range	✓			[22]